Wavelength-dependent magnetic transitions of self-organized iron–aluminum stripes induced by pulsed laser irradiation

Yutaka Yoshida, Seiichi Watanabe, Hideo Kaiju, Junji Nishii, and Kyosuke Yoshimi

Citation: Journal of Applied Physics **117**, 045305 (2015); doi: 10.1063/1.4906523
View online: http://dx.doi.org/10.1063/1.4906523
View Table of Contents: http://scitation.aip.org/content/aip/journal/jap/117/4?ver=pdfcov
Published by the AIP Publishing

Wavelength-dependent magnetic transitions of self-organized iron–aluminum stripes induced by pulsed laser irradiation

Yutaka Yoshida,[1,2,a)] Seiichi Watanabe,[2] Hideo Kaiju,[3] Junji Nishii,[3] and Kyosuke Yoshimi[4]
[1]*Creative Research Institution Sousei, Hokkaido University, Kita-21, Nishi-10, Kita-ku, Sapporo, Hokkaido 001-0021, Japan*
[2]*Center for Advanced Research of Energy and Materials, Faculty of Engineering, Hokkaido University, Kita-8, Nishi-13, Kita-ku, Sapporo, Hokkaido 060-8628, Japan*
[3]*Research Institute for Electronic Science, Hokkaido University, Kita-20, Nishi-10, Kita-ku, Sapporo, Hokkaido 001-0020, Japan*
[4]*Graduate School of Engineering, Tohoku University, Sendai, 6-6-02 Aramaki Aza Aoba, Miyagi 980-8579, Japan*

(Received 26 September 2014; accepted 13 January 2015; published online 26 January 2015)

We investigate the laser wavelength dependence of structural and magnetic transitions on the surface of an iron–aluminum (FeAl) alloy induced by nanosecond pulsed laser irradiation. The formation of self-organized FeAl stripes with a wavelength-dependent period is observed in a local area on the (111)-oriented plane. Focused magneto-optical Kerr effect measurements reveal that the coercivity reaches up to 1.2 kOe with increasing the magnetic field rotation angle, which is estimated from the stripe direction, in FeAl stripes irradiated at 355 nm, and its magnetization reversal can be explained by the domain-wall motion model. On the other hand, the magnetization reversal agrees with the Stoner–Wohlfarth model in FeAl stripes irradiated at 1064 nm. This magnetic transition originates from the B2-to-A2 phase transition in stripe structures and bulk regions. These results indicate that the magnetic transition from the incoherent to coherent mode as well as the structural transformation of stripe patterns can be controlled by the incident laser wavelength. © *2015 AIP Publishing LLC*. [http://dx.doi.org/10.1063/1.4906523]

INTRODUCTION

The fabrication of surface nanostructures using quantum beams, such as electron, ion, and laser beam techniques, has been widely studied because of its potential application for nanostructured and microstructured materials, as well as fundamental research.[1–15] In recent years, such quantum beams have attracted considerable attention for the fabrication of magnetic structures.[16–23] For example, magnetic properties of CoPt multilayers have been controlled by ion irradiation through a lithographically-made resist mask, producing magnetic arrays of 1-μm-wide lines.[16] The disorder-induced magnetism in $Fe_{60}Al_{40}$ alloys has also been controlled by focused ion beam (FIB) or in-parallel broad-beam ion irradiation through lithographed masks, resulting in arrays of sub-100-nm ferromagnetic structures at the surface of nonmagnetic $Fe_{60}Al_{40}$ sheets.[19] Recently, we have demonstrated the formation of unique magnetic nanostructures, such as periodic stripes, network structures, and dot-like protrusion patterns, on the surface of an iron–aluminum (FeAl) alloy by nanosecond pulsed laser irradiation. These nanostructures are attributed to interference and self-organization during laser irradiation. Interestingly, these nanostructures exhibit a paramagnetic to ferromagnetic phase transition, and the enhancement of the coercive force has been observed.[13,14] In this study, we investigate the laser wavelength dependence of structural and magnetic properties on the surface of an FeAl alloy induced by nanosecond pulsed laser irradiation. Moreover, we focus on the magnetic field rotation dependence of the coercive force and discuss the mechanism of the magnetization reversal.

EXPERIMENTAL

An FeAl alloy containing 48% Al was prepared as an ordered polycrystalline substance using an arc-melting technique in an argon gas atmosphere.[24,25] The starting material was a commercially available surface-polished FeAl alloy. The size of the prepared sample for laser irradiation was a thickness of 1 mm and a diameter of 6 mm. Its surface was ultrasonically cleaned before irradiation at room temperature in air using an Nd:YAG pulsed laser (Continuum Co., Ltd. Inlite II) emitting at 355 and 1064 nm with a pulse width of 5–7 ns and a repetition rate of 2 Hz. The laser beam diameter measured 6 mm. The laser irradiation at 355 nm was performed normal to the surface at an average laser energy density of 124 mJ cm^{-2} using 300 laser pulses. The laser irradiation at 1064 nm was performed at an average laser energy density of 992 mJ cm^{-2} using 60 laser pulses. Surface morphologies were analyzed by scanning electron microscopy (SEM; JEOL, JSM-7001F) and atomic force microscopy (AFM; SII NanoTechnology, Nanonavi IIs). Chemical composition and crystalline orientation were examined using SEM–energy dispersive X-ray spectroscopy (EDS) and electron backscattering diffraction patterns, respectively. Structural and chemical analyses were performed by transmission electron microscopy (TEM; JEOL, JEM-2010F) and TEM–EDS (Noran Vantage), respectively.

[a)]Author to whom correspondence should be addressed. Electronic mail: yyoshida@cris.hokudai.ac.jp

The irradiated surface was protected by thicker carbon and tungsten layer depositions before TEM specimen preparation. Cross-sectional TEM specimens were prepared using FIB (Hitachi, FB-2100). Magnetization curves were measured by focused magneto-optical Kerr effect (MOKE) measurements (NEOARK, BH-PI920-HU) under a magnetic field of up to 2 kOe at room temperature. The spot size for the observation of focused MOKE signals was set to 3 μm.

RESULTS AND DISCUSSION

Figures 1(a)–1(e) show SEM images, SEM–EDS maps, and AFM images of the (111)-oriented plane of the FeAl alloy after irradiation at 355 nm. As shown in Fig. 1(a), A stripe pattern is observed along the ⟨110⟩ direction on the near-{111}-oriented plane in a local area exceeding $5 \times 5\ \mu m^2$. EDS mapping of Fe (red, Fig. 1(b)) and Al (blue, Fig. 1(c)) indicates that these elements are uniformly distributed in the pattern. On the other hand, the mapping of oxygen confirms that oxides are aligned in the longitudinal direction of the pattern (yellow, Fig. 1(d)). This indicates that Al oxides form on the slope of FeAl stripes. This behavior has previously been observed in FeAl stripes irradiated at 532 nm.[14] According to AFM images (Fig. 1(e)), the stripe period averages 357 nm, which is almost equivalent to the incident laser wavelength. Average stripe height and width amount to 100 and 206 nm, respectively.

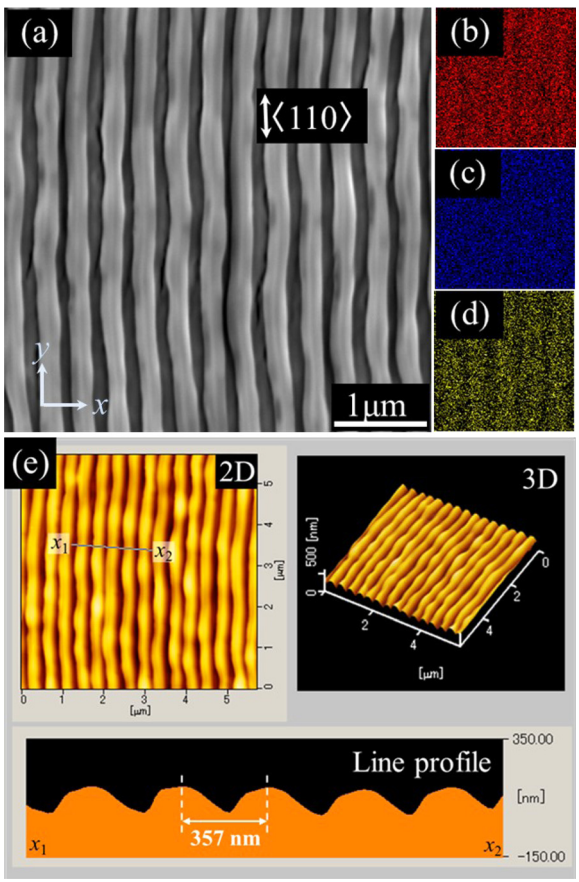

FIG. 1. SEM images of magnetic stripes on FeAl (111) alloy surfaces irradiated for 300 pulses using a 355-nm laser at an average energy density of 124 mJ cm^{-2}. (b)–(d) Elemental distribution of Fe, Al, and O by SEM–EDS at an acceleration voltage of 5 kV. (e) AFM images of the stripe patterns.

Figures 2(a)–2(c) show SEM and TEM images of the (111)-oriented plane of the FeAl alloy after irradiation at 1064 nm. Despite an increase in pulse number from 60 to 1500, no stripe patterns are visible on the irradiated surface at an average energy density of 124 mJ cm^{-2}. An enhanced energy density (992 mJ cm^{-2}) produces stripe patterns along ⟨110⟩ and ⟨112⟩ directions on the {111}-oriented plane. Although the reason for the presence of stripe patterns along these directions is unclear at the present stage, this rotation of stripe pattern is considered to stem from the penetration depth of laser irradiation. As shown in Fig. 2(a), stripe pattern follows the ⟨110⟩ direction on the near-{111}-oriented plane at a local area exceeding $10 \times 10\ \mu m^2$. Figs. 2(b) and 2(c) show cross-sectional TEM images acquired along the x_1–x_2 direction indicated in Fig. 2(a). The average stripe period equals 1067 nm, which is quasi-similar to the incident laser wavelength. The brightly contrasted surface section (green arrow, *l1*), stripe structure (red, *l2*), and the bulk (yellow, *l3*) are readily recognizable in Fig. 2(c). Average stripe height and width amount to 160 and 653 nm, respectively. Figures 2(d) and 2(e) show the diffraction patterns of the stripe structure (labeled *l2*) and bulk (*l3*) in Fig. 2(c). Surface stripe and bulk regions present the same spot angles in the diffraction patterns, consistent with an epitaxial stripe structure. However, these spots do not indicate superlattice (B2-type) structures. This means that the surface stripe and bulk regions are transformed from an ordered B2 phase to a disordered A2 phase by the annealing effect of the 1064-nm laser. This structural transition in the bulk regions results from a strong thermal effect because the penetration depth for a 1064-nm laser is greater than that for 355- and 532-nm lasers. The depth of bulk after 1064 nm laser irradiation was more than about 8 μm, and all regions in TEM sample fabricated by FIB system were confirmed A2-type structure. The stripe structure after 1064-nm laser irradiation is expected the behavior to magnetic shape anisotropy. Figures 2(f)–2(h) show TEM–EDS results for surface section (arrow *l1*), stripe structure (*l2*), and bulk (*l3*) in Fig. 2(c). The brightly contrasted section primarily consists of Al and O, whereas stripe and bulk structures both comprise Fe and Al in similar proportions, consistent with the behavior observed for FeAl stripes irradiated at 355 and 532 nm.

The magnetic properties in the FeAl alloy are investigated by measuring the MOKE of the self-organized stripes at each laser irradiation wavelength. Figure 3 shows the magnetic field rotation dependence of the magnetization curves for FeAl stripes after irradiation at 355 and 1064 nm. Here, the field rotation angle θ is defined as the angle between the magnetic field and the longitudinal direction of the stripe patterns. The coercive force increases with increasing the angle θ in FeAl stripes irradiated at 355 nm. In contrast, the coercive force decreases to 0 Oe when the angle θ approaches 90° in FeAl stripes irradiated at 1064 nm.

Figure 4 shows the coercive force as a function of the angle θ in FeAl stripes irradiated at 355, 532,[14] and 1064 nm. Experimental data are plotted with the calculation results obtained using the domain wall (DW; blue and green solid

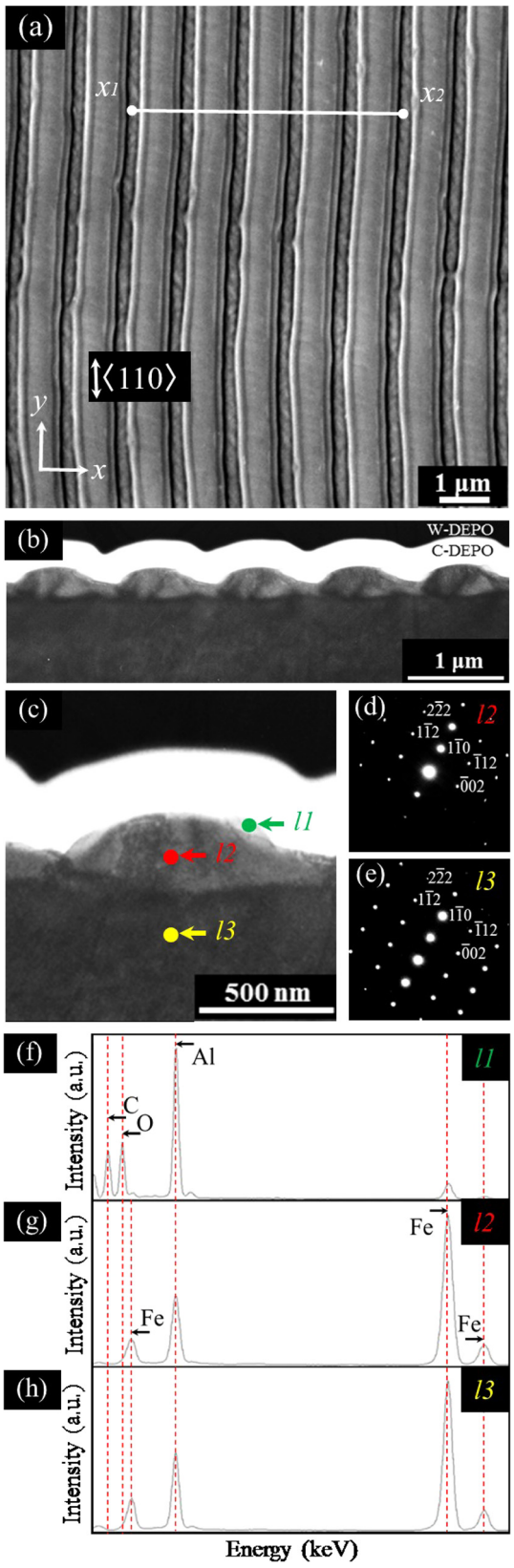

FIG. 2. SEM images of stripe patterns formed on FeAl (111) alloy surfaces irradiated for 60 pulses using a 1064-nm wavelength laser at an average energy density of 992 mJ cm^{-2}. (b) and (c) Cross-sectional TEM images acquired along the x_1–x_2 direction shown in (a). (d) and (e) Diffraction patterns examined in the labeled regions *l2* and *l3* shown in (c). (f)–(h) TEM–EDS analyses at points marked by the arrows *l1*, *l2*, and *l3* shown in (c). The upper layers of the stripe structure have carbon-deposition (C-DEPO) and tungsten-deposition (W-DEPO) layers, as shown in (b) and (c). The C and W layers are deposited for damage protection from gallium ion beam used in the FIB process.

lines) motion and Stoner–Wohlfarth (SW) motion models (red solid line). In the DW motion model, the coercive force H_c is given as $H_{c0}/\cos\theta$, where H_{c0} is the coercive force at $\theta = 0°$ for $0 \le \theta \le 90°$.[23] This means that the magnetization reversal is mainly driven by the magnetic field component parallel to the stripe lines. In the SW model, the angle θ and the coercive force H_c are related using the equation as follows:[26]

$$\sin 2\theta = \begin{cases} \left(\frac{H_{c0}}{2H_c}\right)^2 \left(\frac{4-(2H_c/H_{c0})^2}{3}\right) & 0 \le \theta \le 45° \\ 2H_c/H_{c0} & 45° < \theta \le 90°. \end{cases} \quad (1)$$

This means that the magnetization results from coherent rotation. The coercive force reaches a maximum of 1.2 kOe at a field rotation angle of 88° in FeAl stripes irradiated at 355 nm as shown in Fig. 4. Experimental results at 355 and 532 nm agree with the DW motion model, suggesting that the magnetization reversal originates from the DW pinning in single domain which is observed by a magnetic force microscopy (not shown), and thus, the magnetization rotates incoherently. This is consistent with the observations of some "jump" fields (black arrows, Fig. 3(a)).[27] These results also agree with structural analysis showing that the surface stripe structures undergo a B2 to A2 phase transition, as well as the results in FeAl stripes irradiated at 532 nm. The magnetic property of A2-type thin film on B2 phase is strongly affected by Al oxide. Experimental results at 1064 nm show a good agreement with the SW model. This indicates that the magnetization reversal is only attributed to the uniaxial magnetic shape anisotropy, and thus, the magnetization rotates coherently. This demonstrates the magnetization reversal transitions from the incoherent to coherent rotation mode when the incident laser wavelength increases. The magnetic transition implies originate from a magnetic pinning site. The SEM–EDS mapping (Figs. 1(b)–1(d)) and the cross-sectional TEM image and EDS analysis (Figs. 2(f)–2(h)) show that Al oxide is present on the slope of FeAl stripes and acts as a magnetic pinning site. This behavior has been already reported in FeAl stripes irradiated at 532 nm. Consequently, the effect of magnetic pinning in FeAl stripes irradiated at 1064 nm is expected to be weaker than that of FeAl stripes irradiated at 355 and 532 nm. This is because of FeAl stripes irradiated at 1064 nm are wider than that at 355 and 532 nm, as shown in Figs. 1(a) and 2(a). The reduced ratio of Al oxide to FeAl leads to weak magnetic pinning in single domain. Moreover, the structural analysis (Figs. 2(d) and 2(e)) shows that the bulk and surface regions exhibit the disordered A2 phase in FeAl stripes irradiated at 1064 nm as a result of a strong annealing effect. This effect also weakens magnetic pinning, i.e., the uniaxial shape anisotropy is predominant in the magnetic anisotropy.

SUMMARY

Self-organized FeAl stripes with a wavelength-dependent period can be formed locally on the (111)-oriented plane by

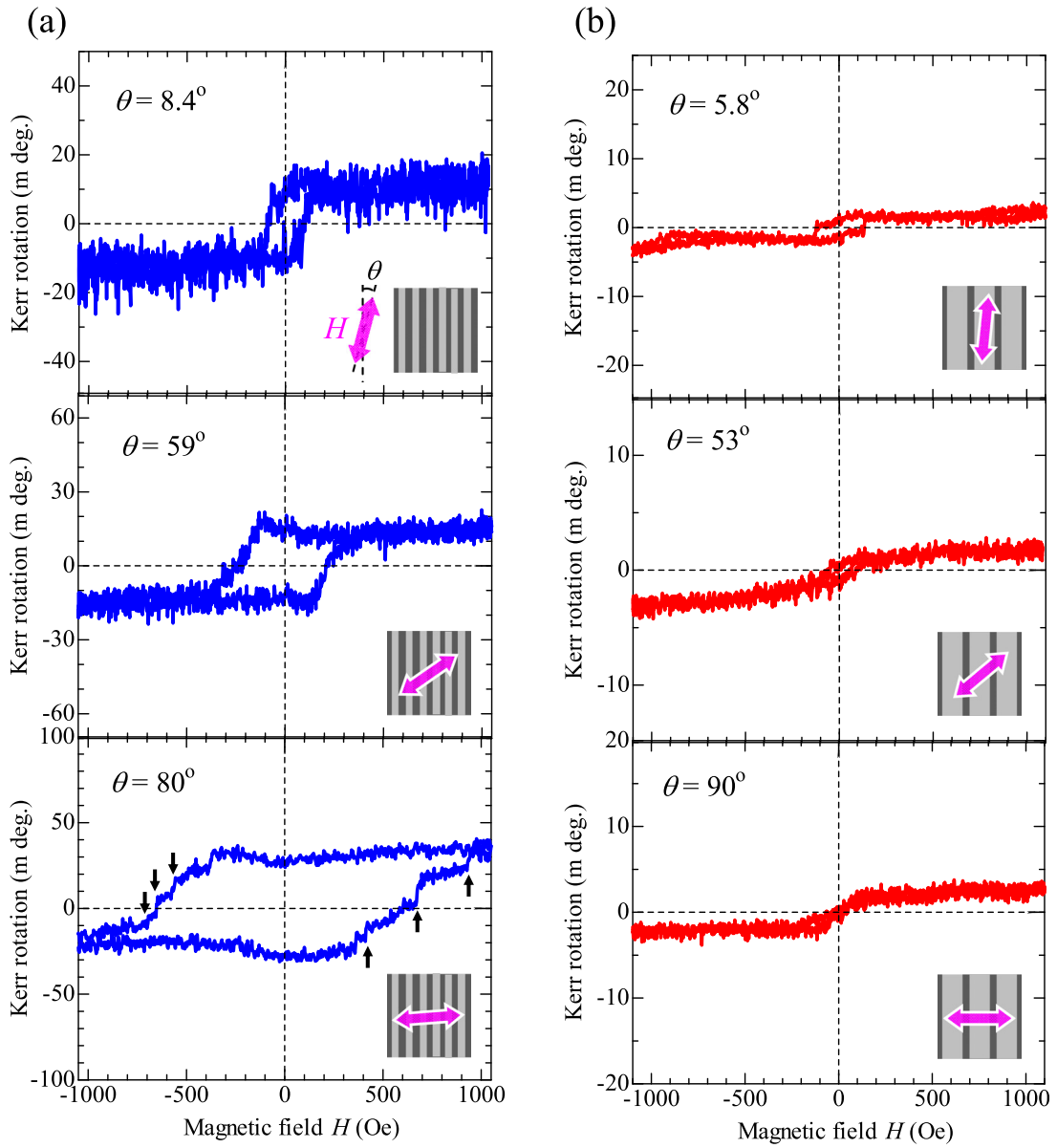

FIG. 3. Magnetic field rotation dependence of the magnetization curves for FeAl stripes after laser irradiation at (a) 355 and (b) 1064 nm.

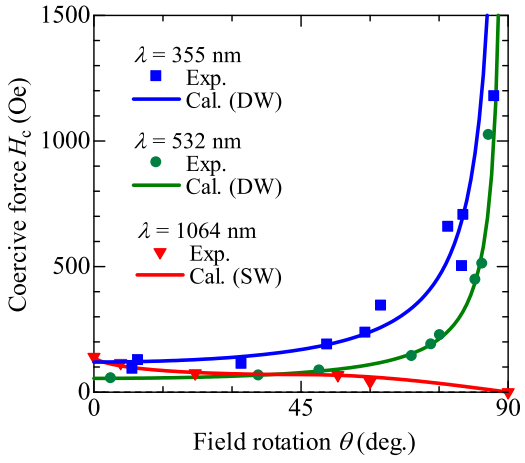

FIG. 4. Coercive force as a function of the magnetic field rotation angle for FeAl stripes irradiated at 355, 532,[14] and 1064 nm. Blue and red solid lines correspond to the fit to the DW motion and SW model, respectively.

nanosecond pulsed laser irradiation. Focused MOKE measurements reveal that the coercivity reaches up to 1.2 kOe at a magnetic field rotation angle of 88° in FeAl stripes irradiated at 355 nm. Furthermore, the magnetic transition from the incoherent to coherent rotation mode can be observed when the laser wavelength increases, typically to 1064 nm, because stripe structures and bulk regions undergo a B2-to-A2 phase transformation in FeAl stripes irradiated at 1064 nm. The magnetic transition phenomenon is crucial for fundamental research and potential applications in hard or soft magnetic materials, such as magnetic storage materials/devices and sensors.

ACKNOWLEDGMENTS

The authors would like to express their sincere appreciation to Professor Osamu Kitakami of Tohoku University, as well as Yasutaka Matsuo, Tamaki Shibayama, Norihumi Sakaguchi, Shigeo Yatsu, Dr. Takashi Endo, Mr.

Kenji Ohkubo, and Mrs. Mika Yamamoto, and Junko Iwasaki of Hokkaido University for their technical assistance and helpful discussions.

[1]H. Brune, M. Giovanini, K. Broman, and K. Kern, Nature **394**, 451 (1998).
[2]Z. Yang and S. Watanabe, Acta Mater. **61**, 2966 (2013).
[3]M. Birnbaum, J. Appl. Phys. **36**, 3688 (1965).
[4]J. E. Sipe, J. F. Young, J. S. Preston, and H. M. Van Driel, Phys. Rev. B **27**, 1141 (1983).
[5]J. F. Young, J. S. Preston, H. M. Van Driel, and J. E. Sipe, Phys. Rev. B **27**, 1155 (1983).
[6]F. Costache, M. Henyk, and J. Reif, Appl. Surf. Sci. **208**, 486 (2003).
[7]O. Varlamova, F. Costache, J. Reif, and M. Bestehorn, Appl. Surf. Sci. **252**, 4702 (2006).
[8]A. Lasagni, C. Holzapfel, and F. Mücklich, Adv. Energy Mater. **7**, 487 (2005).
[9]H.-C. Kim, H. Reinhardt, P. Hillebrecht, and N. A. Hampp, Adv. Mater. **24**, 1994 (2012).
[10]H. Reinhardt, H.-C. Kim, C. Pietzonka, J. Kruempelmann, B. Harbrecht, B. Roling, and N. A. Hampp, Adv. Mater. **25**, 3313 (2013).
[11]S. Watanabe, Y. Yoshida, S. Kayashima, S. Yatsu, M. Kawai, and T. Kato, J. Appl. Phys. **108**, 103510 (2010).
[12]Y. Yoshida, S. Watanabe, Y. Nishijima, K. Ueno, H. Misawa, and T. Kato, Nanotechnology **22**, 375607 (2011).
[13]Y. Yoshida, K. Oosawa, S. Watanabe, H. Kaiju, K. Kondo, A. Ishibashi, and K. Yoshimi, Appl. Phys. Lett. **102**, 183109 (2013).
[14]H. Kaiju, Y. Yoshida, S. Watanabe, K. Kondo, A. Ishibashi, and K. Yoshimi, J. Appl. Phys. **115**, 17B901 (2014).
[15]Y. Yoshida, K. Oosawa, J. Wajima, S. Watanabe, Y. Matsuo, and T. Kato, Appl. Surf. Sci. **307**, 24 (2014).
[16]C. Chappert, H. Bernas, J. Ferre, V. Kottler, J. P. Jamet, Y. Chen, E. Cambril, T. Devolder, F. Rousseaux, V. Mathet, and H. Launois, Science **280**, 1919 (1998).
[17]K. Liu, J. Nogués, C. Leighton, H. Masuda, K. Nishio, I. V. Roshchin, and I. K. Schuller, Appl. Phys. Lett. **81**, 4434 (2002).
[18]J. Sort, A. Concustell, E. Menéndez, S. Suriñach, K. V. Rao, S. C. Deevi, M. D. Baró, and J. Nogués, Adv. Mater. **18**, 1717 (2006).
[19]E. Menéndez, M. O. Liedke, J. Fassbender, T. Gemming, A. Weber, L. J. Heyderman, K. V. Rao, S. C. Deevi, S. Suriñach, M. D. Baró, J. Sort, and J. Nogués, Small **5**, 229 (2009).
[20]D. Oshima, T. Kato, S. Iwata, and S. Tsunashima, IEEE Trans. Magn. **49**, 3608 (2013).
[21]A. Varea, E. Menéndez, J. Montserrat, E. Lora-Tamayo, A. Weber, L. J. Heyderman, S. C. Deevi, K. V. Rao, S. Suriñach, M. D. Baró, K. S. Buchanan, J. Nogués, and J. Sort, J. Appl. Phys. **109**, 093918 (2011).
[22]X. Yao, U. Wiedwald, M. Trautvetter, and P. Ziemann, J. Appl. Phys. **115**, 023507 (2014).
[23]J. I. Martín, M. Vélez, R. Morales, J. M. Alameda, J. V. Anguita, F. Briones, and J. L. Vicent, J. Magn. Magn. Mater. **249**, 156 (2002).
[24]M. Zhao, K. Yoshimi, K. Maruyama, and K. Yubuta, Acta Mater. **64**, 382 (2014).
[25]M. Zhao, K. Yoshimi, J. Nakayama, K. Yubuta, and T. Sugawara, Scr. Mater. **82**, 37 (2014).
[26]E. C. Stoner and E. P. Wohlfarth, Trans. R. Soc. London, Ser. A **240**, 599 (1948).
[27]A. O. Adeyeye, J. A. C. Bland, C. Daboo, and D. G. Hasko, Phys. Rev. B **56**, 3265 (1997).